The Role of Ionic Backbones in RNA Structure: An Unusually Stable Non-Watson−Crick Duplex of a Nonionic Analog in an Apolar Medium

Christoph Steinbeck*,† and Clemens Richert*

Contribution from the Department of Chemistry, Tufts University, 62 Talbot Avenue, Medford, Massachusetts 02155

Received May 26, 1998

Abstract: The solution structure of a dimethylenesulfone-linked analogue of the RNA dimer U_PC was determined using two-dimensional NMR and restrained molecular dynamics. In $CDCl_3$, the RNA analogue forms a parallel duplex with a single U:U base pair and roughly antiparallel orientation of the two ribose rings within each strand. A hydrogen bonding network stabilizing this duplex was indirectly deduced from the NMR data. Besides the two-pronged hydrogen bonding between the uridines, this network includes two hydrogen bonds from the ribose hydroxyls of one strand to O2 of the cytosine bases of the opposite strand, and intrastrand hydrogen bonds from the 2′ hydroxyls of the 5′-terminal residues to hydroxyls of the 3′-terminal residue. The melting point of the duplex determined via NMR chemical shift analysis was found to be 91 °C for a 11 mM solution in 1,1,2,2-tetrachloroethane-d_2. Based on van't Hoff analysis of the available UV melting data in 1,2-dichloroethane, duplex formation is associated with a $\Delta S°$ of −47 cal K^{-1} mol^{-1} and a $\Delta H°$ of −22 kcal mol^{-1}. The observation that an RNA analogue rendered nonionic and removed from an aqueous environment forms an exceptionally stable non-Watson−Crick duplex with backbone-to-nucleobase and backbone-to-backbone hydrogen bonds suggests that a charged backbone and the solubility in aqueous medium that it conveys are important for limiting the repertoire of strand−strand interactions of oligoribonucleotides.

Introduction

Nucleic acids with phosphodiester backbones dissolved in aqueous media bear the genetic information of all known forms of life, usually as Watson−Crick paired duplexes with a complementary strand. Modified nucleic acids have recently become available, mostly as the result of a quest for antisense agents with improved bioavailability.[1] Comparing the molecular recognition properties of such modified nucleic acids to those of their natural counterparts offers one approach to rationalizing why nature selected nucleic acids in aqueous medium as genetic material.[2] Among the backbone-modifications described to date, the dimethylenesulfone replacement of phosphodiesters is one of the few, for which synthetic methodology is available for analogues of both DNA[3] and RNA.[4]

The dimethylenesulfone-linked RNA analogues show some unusual recognition properties. An X-ray crystal structure demonstrated the ability of the RNA analogues to form canonical Watson−Crick duplexes.[5] From crystals grown at elevated temperature it is clear that even in the single-stranded state a largely RNA-like conformation is maintained.[6] Yet, DNA:RNA duplexes containing dimethylenesulfone linkages melt at lower temperatures than those of their unmodified control sequences, with a single sulfone linkage inducing a melting point depression of up to 16 °C.[7] This lowered stability was unexpected, since nonionic analogues, whose duplexes are not tempered by the charge repulsion between phosphodiesters, should show increased duplex stability. The all-sulfone analogue of the RNA octamer 5′-AUGGUCAU-3′ does, in fact, not bind to complementary oligonucleotides at all, but forms a unimolecular structure that melts with more than 100% hyperchromicity.[4] This suggests that besides canonical Watson−Crick duplexes, alternative, non-Watson−Crick low-energy structures are available to nonionic RNA analogues. Here we report the first three-dimensional structure of a dimethylene sulfone-linked RNA analogue forming a non-Watson−Crick structure.

Results and Discussion

The structure was solved for an analogue of the RNA dimer 5′-U_PC-3′ via two-dimensional NMR and molecular dynamics. The analogue ($U_{SO2}C$)[8] bears two noninterfering solubilizing

† Current address: Max-Planck-Institut für Chemische Ökologie, D-07745 Jena, Germany.

(1) Selected reviews: (a) Uhlmann, E.; Peyman, A. *Chem. Rev.* **1990**, *90*, 544−584. (b) Milligan, J. F.; Matteucci, M. D.; Martin, J. C. *J. Med. Chem.* **1993**, *36*, 1923−1937. (c) Saghvi, Y. S., Cook, P. D., Eds.; *Carbohydrate Modifications in Antisense Research*; ACS Symposium Series; American Chemical Society: Washington, DC, 1994; pp. 1−22. (d) DeMesmaeker, A.; Haener, R.; Martin, P.; Moser, H. E. *Acc. Chem. Res.* **1995**, *28*, 366−374. (e) Hunziker, J.; Leumann, C. In *Modern Synthetic Methods*, Ernst, B., Leumann, C., Eds.; Verlag Helvetica Chimica Acta: Basel, 1995; pp 333−417. (f) Agrawal, S.; Iyer, R. P. *Pharmacol. Ther.* **1997**, *76*, 151−160.

(2) Eschenmoser, A.; Loewenthal, E. *Chem. Soc. Rev.* **1992**, *21*, 1−16.

(3) (a) Blättler, M. O.; Wenz, C.; Pingoud, A.; Benner, S. A. *J. Am. Chem. Soc.* **1998**, *120*, 2674−2675. (b) Huang, Z.; Schneider, K. C.; Benner, S. A. *J. Org. Chem.* **1991**, *56*, 3869−3882. (c) Schneider, K. C.; Benner, S. A. *Tetrahedron Lett.* **1990**, *31*, 335−338.

(4) Richert, C.; Roughton, A. L.; Benner, S. A. *J. Am. Chem. Soc.* **1996**, *118*, 4518−4531.

(5) (a) Roughton, A. L.; Portmann, S.; Benner, S. A.; Egli, M. *J. Am. Chem. Soc.* **1995**, *117*, 7249−7250. (b) Egli, M. *Angew. Chem.* **1996**, *108*, 2021−2036, *Angew. Chem., Int. Ed. Engl.* **1996**, *35*, 1894−1909.

(6) Hyrup, B.; Richert, C.; Schulte-Herbrüggen, T.; Benner, S. A.; Egli, M. *Nucleic Acids Res.* **1995**, *23*, 2427−2433.

(7) Baeschlin, D. K.; Hyrup, B.; Benner, S. A.; Richert, C. *J. Org. Chem.* **1996**, *61*, 7620−7626.

(8) Compound **35** in ref 4.

10.1021/ja9817951 CCC: $15.00
Published on Web 11/03/1998

groups, one at the 5′-terminus, and one at the side of the cytosine ring that, in canonical duplexes, faces into the major groove.[9] Without these two solubilizing groups, the dinucleotide does not have sufficient solubility for multidimensional NMR in either water or common organic solvents. With these two lipophilic groups, however, the molecule dissolves sufficiently well to produce millimolar solutions in a number of organic solvents, but not in water. Judged by chemical shifts, it forms a single, stably folded structure in deuteriochloroform and 1,1,2,2-tetrachloroethane-d_2, both in the absence and the presence of water. NMR spectra of the organic portion of a two-phase system of $CDCl_3$ and D_2O also do not indicate complex dissociation when heated to 58 °C, i.e., 3 °C below the boiling point of chloroform (see Supporting Information). The only discernible spectral change associated with heating the water-saturated solution is a slight ($\leq$0.2 ppm) upfield shift of one of the two H5′ resonances of the uridine residue. In CD_3CN, $U_{SO2}C$ shows more than one set of resonances, with several chemical shifts of the predominant set close to those observed in the halogenated solvents. In a mixture of dimethyl sulfoxide-d_6 and D_2O (7:2), one set of chemical shifts consistent with an unfolded monomeric form is observed.

The three-dimensional structure of $U_{SO2}C$ was solved on the basis of spectra acquired in $CDCl_3$. Cross-peaks in NOESY[10] and ROESY[11] spectra indicated a tightly interwoven symmetrical duplex, requiring implementation of Nilges' simulated annealing protocol for symmetrical dimers.[12] With this and a set of 36 distance constraints, a parallel duplex was obtained as the only structure in agreement with the experimental data. This structure was refined in an iterative process by including increasing numbers of hydrogen bonding, base pair planarity, and repulsive constraints in consecutive molecular dynamics calculations, as described in detail in the Experimental Section and summarized in Table 1. The force field minimized average of the resulting set of constraint violation-free structures shows good agreement between back-calculated and experimental NOESY spectra (Figure 1).

The symmetrical duplex is tightly folded, except for the two protecting groups, which protrude from the core of the duplex and are not involved in hydrogen bonding (Figure 2). The solubilizing group at the 5′-terminus is fully disordered and does not show internucleoside NOEs. The benzoyl group at position 4 of the cytosine base has one ortho-hydrogen of its phenyl ring within 2.0 Å of H3′ of the uridine residue, but does not pack tightly against the surface of this residue. It is tethered to the nucleobase by an amide group with a substantial rotational barrier and is therefore not expected to be disordered. The duplex itself is stabilized by a single base pair, together with backbone-to-backbone and backbone-to-nucleobase hydrogen bonds (Figure 3). The base pairing (Figure 3a) occurs between the two uridine residues in a type XIII (according to Saenger)[13] or type I (according to Weisz et al.)[14] arrangement. All backbone OH groups act as hydrogen bond donors. The acceptor for both the uridinyl 2′-hydroxyl and the cytidinyl 2′-hydroxyl is the carbonyl oxygen at position 2 of the cytidine residue on the opposite strand (Figure 3c). This unusual self-pairing between the backbone hydroxyls and the cytidine carbonyl oxygen is made possible by a backbone-fold that puts the two ribose rings within each strand in roughly antiparallel orientations. The backbone-fold appears to be stabilized by an intramolecular hydrogen bond from the cytidinyl 3′′-hydroxyl to the uridinyl 2′-hydroxyl (Figure 3b). Among the resulting backbone torsion angles, the values for β and γ are the most unexpected, on the basis of previous sulfone structures (Table 2). Extension of the duplex by additional base pairs is conceivable, as the 5′-termini with their U:U base pair could, in principle, be a template for the assembly of longer parallel pyrimidine:pyrimidine duplexes (Figure 4).

Table 1. Summary of the Restraints[a] Used for Molecular Dynamics Calculations and Data on the Refined Set of Structures

NOE restraints	
total number	36
intermolecular	10
intra/intermolecular[b]	18
restraints per residue	18
dihedral angle restraints	2
hydrogen bonds	4
repulsive restraints	3
base pair planarity restraints	1
refinement statistics for 10 final lowest energy structures	
rmsd from average[c]	0.49 Å
pairwise rmsd of coordinates[c]	0.94 Å
pairwise rmsd of angles[c]	1.5°
pairwise rmsd of bond lengths[c]	0.02 Å
energy	488 ± 11 kcal/mol
restraint violation	
NOE violations	0
dihedral angle violations[d]	0
H-bond violations	0
repulsive restraint violations	0
deviation from ideal geometry	
bond distances	<0.027 Å
bond angles	<3°

[a] Due to the symmetrical nature of the duplex, all constraints except the base pair planarity constraints were applied to both strands, formally resulting in twice the number of constraints given. [b] Used with mixed energy functions (ref 12). [c] Without solubilizing groups. [d] Deviations >5°.

Heating solutions of the nonionic RNA analogue in chloroform to within 5 °C of the boiling point did not result in spectroscopically noticeable changes. Only when higher boiling organic solvents were employed could duplex dissociation be observed. UV-spectra in 1,2-dichloroethane, acquired in the concentration range of 19 to 70 μM, showed hyperchromicity upon heating, with a concentration-dependent melting point and a smaller hyperchromicity (4−5%) than for Watson−Crick paired duplexes (Figure 5). The small hyperchromicity limits the concentration range in which UV melting points can be accurately determined. A plot of the available reciprocal melting points versus the natural log of the concentration yields $\Delta S^\circ = -47$ cal K^{-1} mol^{-1} and $\Delta H^\circ = -22$ kcal mol^{-1} for the association of the two strands in $C_2H_4Cl_2$. Melting was also observed in ^{1}H NMR spectra acquired in 1,1,2,2-tetrachloroethane-d_2 in the temperature range of 50−120 °C. A DQF-COSY[15] spectrum acquired at 120 °C allowed assignment of most resonances in the high-temperature spectra. Nucleobase signals and a number of backbone signals started broadening at 70 °C and sharpened again at 100 °C at chemical shift values similar to those of monomeric control compounds. Signals for

(9) Christensen, L.; Hansen, H. F.; Koch, T.; Nielsen, P. E. *Nucleic Acids Res.* **1998**, *26*, 2735−2739.

(10) Kumar, A.; Ernst, R. R.; Wüthrich, K. *Biochem. Biophys. Res. Commun.* **1980**, *95*, 1−6.

(11) (a) Bothner-By, A. A.; Stephens, R. L.; Lee, J. M.; Warren, C. D.; Jeanloz, R. W. *J. Am. Chem. Soc.* **1984**, *106*, 811−813. (b) Bax, A.; Davis, D. G. *J. Magn. Res.* **1985**, *63*, 207−213.

(12) (a) Nilges, M. *Proteins* **1993**, *17*, 297−309. (b) Nilges, M. *J. Mol. Biol.* **1995**, *245*, 645−650.

(13) Saenger, W. *Principles of Nucleic Acid Structure*; Springer, New York: 1984; p 120.

(14) Weisz, K.; Jähnchen, J.; Limbach, H.-H. *J. Am. Chem. Soc.* **1997**, *119*, 6436−6437.

(15) Piantini, U.; Sørensen, O. W.; Ernst, R. R. *J. Am. Chem. Soc.* **1982**, *104*, 6800−6801.

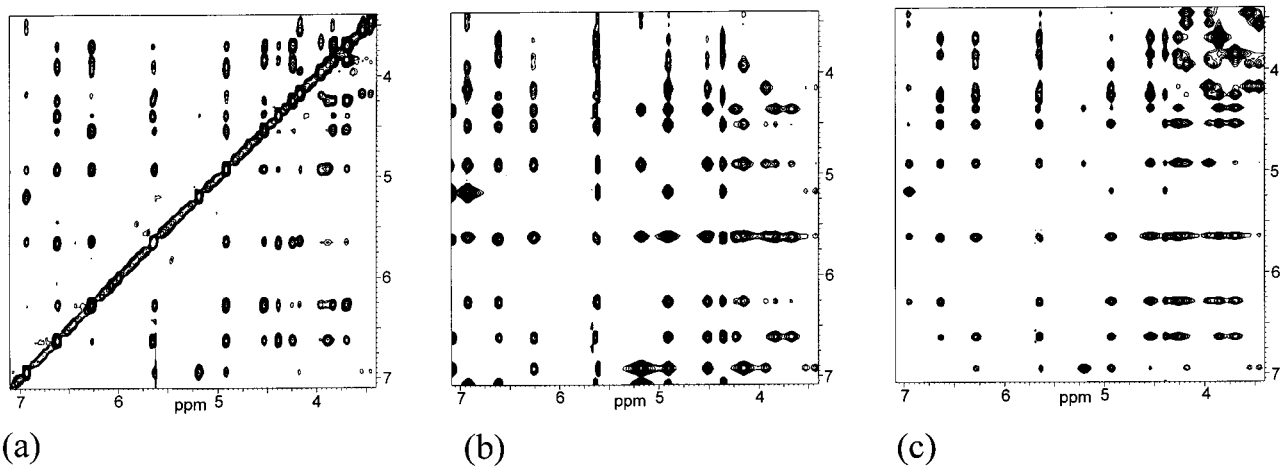

Figure 1. Comparison of the core regions of experimental and back-calculated NOESY spectra. (a) Experimental NOESY spectrum of $U_{SO_2}C$ in $CDCl_3$ (500 MHz) at 250 ms mixing time. (b) Back-calculated NOESY spectrum of the average of the ten lowest energy structures of $U_{SO_2}C$ obtained from restrained molecular dynamics with NOE-based distance constraints only. (c) Same as (b), except that constraints indirectly determined from the NMR data (hydrogen bonding, U:U base pair planarity, and repulsive constraints) were included. Back-calculations were performed on the 50-step force field minimized average structures with X-PLOR[22] using the two spin approximation. Back-calculated spectra do not contain a diagonal. Plots were produced with GIFA.[21]

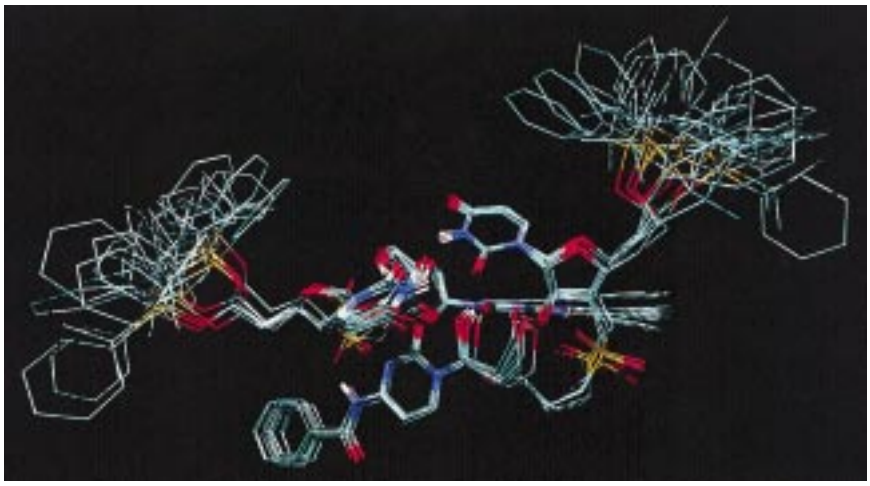

Figure 2. Overlay of 10 violation-free structures of the duplex of $U_{SO_2}C$ obtained from molecular dynamics. Only hydrogens attached to heteroatoms are shown for clarity. Color code: green, carbon; white, hydrogen; blue, nitrogen; red, oxygen; yellow, sulfur or silicon.

exchangeable hydrogens remained broad above 100 °C, most probably due to rapid exchange with residual water in the solvent. Figure 5 shows the chemical shift changes for the H-5 of the uridine residue. The melting point determined graphically from this is 91 °C, in satisfactory agreement with that extrapolated from the fit to the UV-data for this 11 mM solution, validating the above-given thermodynamic parameters.

Several conclusions can be drawn from these results. On an energetic level, the structure formed by this analogue of an RNA dimer is notable for being unusually stable. Since hydrophobic and ionic interactions are absent in the complex, the solvents are good competitors for van der Waals interactions, and base-stacking is less extensive than in Watson−Crick duplexes, the hydrogen bonds are most probably the main driving force for the molecular assembly. Among these, the hydrogen bonds involving the backbone hydroxyl groups seem particularly strong, since $\Delta H°$ for the association of U:U base pairs in chloroform has been determined to be as low as 4.3 kcal mol^{-1}.[16] The strength of the intermolecular hydrogen bonds in a hydrophobic environment, together with the rigidifying effect of the intramolecular hydrogen bond, may explain why duplex formation occurs for so short an oligonucleotide.

Second, this structure is interesting in the context of some of the unexpected properties of antisense agents with a nonionic replacement for the phosphodiester moiety, since it demonstrates that there can be low-energy structures that compete with Watson−Crick base pairing. Populating these alternative structures can shift binding equilibria away from Watson−Crick duplexes, lowering the affinity for target strands. It should be noted, however, that RNA is known to form single stranded structures with a greater propensity than DNA. It is therefore likely that the identification of putative single-stranded structures formed by nonionic analogues of DNA will require a more extensive search of structure space than for our nonionic RNA analogues. Unspecific non-Watson−Crick interactions between strands, on the other hand, often in the form of aggregation, are quite common among nonionic DNA analogues. PNAs, for example, have been noted to aggregate,[17] and the desire to suppress this property has been one incentive for synthesizing PNA chimera, either with charged amino acid residues[18] or with DNA oligomers.[19]

(16) Kyogoku, Y.; Lord, R. C.; Rich, A. *Biochim. Biophys. Acta* **1969**, *179*, 10−17.
(17) Egholm, P., Ph.D. Thesis, University of Copenhagen, 1992.

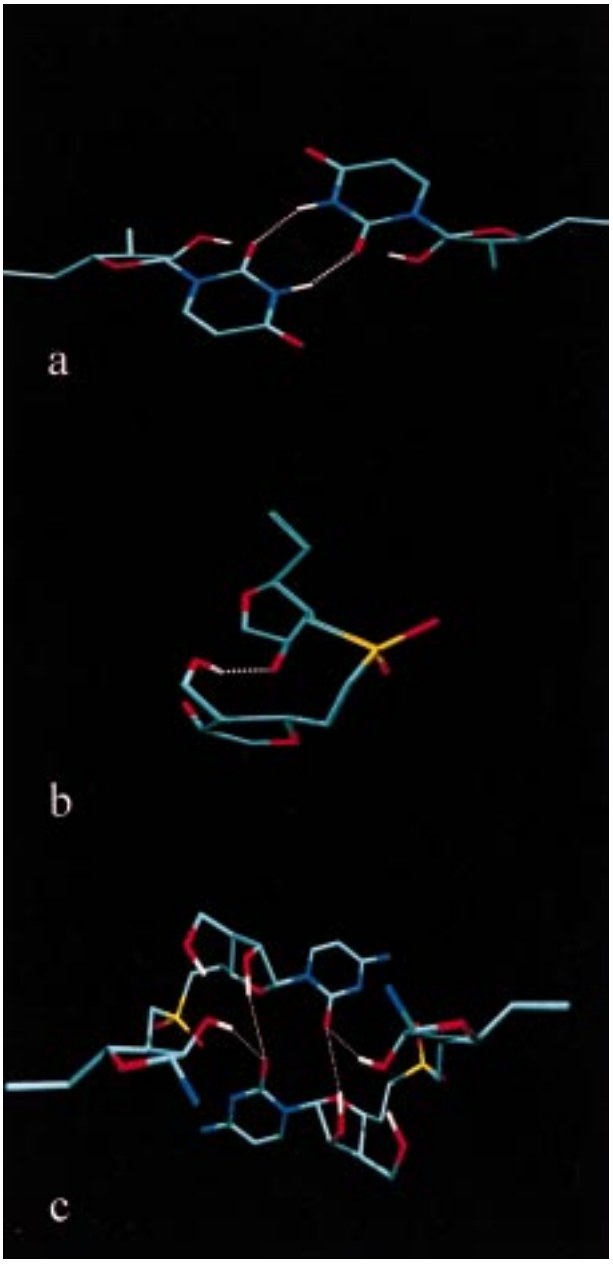

Figure 3. Selected details of the duplex of $U_{SO_2}C$. Assigned hydrogen bonds are highlighted with broken white lines. (a) U:U base pair, (b) intramolecular hydrogen bond, (c) backbone-to-nucleobase hydrogen bonds. Same color code as for Figure 2.

Table 2. Comparison of Selected Torsion Angles in $U_{SO_2}C$ (this work) and Related Compounds

sequence	χ(U)	ϵ(U)	ζ(U)	α(C)	β(C)	γ(C)	χ(C)[a]
$U_{SO_2}C$[b]	−151	−139	−100	−45	96	−156	−138
$G_{SO_2}C$[c,d]	−178	−140	−66	−58	−179	44	−170
$A_{SO_2}U$[c,e,f]	−169	−153	177	−168	−165	179	−171
-U_PC-[g]	−154	−136	−80	−46	148	52	−163

[a] See ref 13 for definition of torsion angles. [b] Average of both strands. [c] Angles from 3′-terminal and 5′-terminal residues equivalent to U and C. [d] From ref 5a. [e] Average from two molecules in the asymmetric unit. [f] From ref 6. [g] Residues 38/39 in the crystal structure of *r*(UAAGGAGGUGAU)·*r*(AUCACCUCCUUA), from ref 28.

Third, the $U_{SO_2}C$ duplex corroborates the assumption that in the absence of the repulsive effect of phosphate groups, oligonucleotides behave similarly to peptides,[4] since the intramolecular hydrogen bond stabilizing the backbone-fold is analogous to those stabilizing α-helices in proteins. Finally, our results support the notion[4] that phosphodiester groups found in natural RNA secure the unambiguous readability of genetic material, as they seem to prevent strong non-Watson−Crick interactions that can predominate in lipophilic environments. Maybe Nature chose phosphates not only to stabilize genetic material against hydrolysis and to retain it within lipid membranes[20] but also to limit its repertoire of strand−strand interactions, thereby permitting it to display rule-based molecular recognition.

Experimental Section

NMR Spectroscopy. NOESY spectra of $U_{SO_2}C$ in $CDCl_3$ (4−40 mM) at 75 ms and 250 ms mixing time were acquired at 300 K and 500 MHz in States-TPPI mode with 512 T_1 increments and 2k real data points, together with ROESY control spectra. Resonances assignment, based on DQF-COSY, DEPT, and HETCOR spectra, has previously been reported (ref 4). Spectra were zero-filled to 2k × 2k and processed with integration of cross-peaks using GIFA.[21]

Molecular Dynamics. Restrained molecular dynamics, based on simulated annealing, were performed with X-PLOR[22] version 3.1 using 36 distance constraints (strong, 1.8−2.7 Å; medium, 1.8−3.7 Å; and weak, 1.8−5.0 Å) obtained from the NOESY spectrum at 75 ms (ensuring minimal spin-diffusion effects) and calibrated on known distances (H5 to H6 of U and C). Distance constraints were divided into two groups, those unequivocally assignable to intra- or interstrand magnetization transfer and those without such an assignment. Those from the latter category were included in all of the calculations with mixed energy functions.[12] Correct orientation of the pairing strands was achieved in initial calculations with 14 distance constraints from the former and seven from the latter category. After introducing the remaining 15 nontrivial NOE-derived constraints and a coupling-constant-based[23] dihedral angle constraint for each ribose, a set of less diverse structures emerged, but only two of the obtained structures (4% of the total of 50) satisfied the criteria of the stringent acceptance protocol (Table 1). A back-calculated NOESY spectrum of the average of the 10 lowest energy structures showed limited agreement with the experimental spectrum (Figure 1a and b).

Refinement involved molecular dynamics calculations with an increasing number of constraints derived indirectly from NMR data and from spatial proximity in the unrefined structure set. First, possible pairs of hydrogen bond donors and acceptors were identified by sampling distances between potential donor protons and acceptor heteroatoms. All three ribose hydroxyls and the NH of uracil were among the former since their resonances show >0.7 ppm low-field shift compared to monomeric derivatives.[24] Acceptor sampling included heteroatoms of riboses and nucleobases, as well as the oxygens of the sulfone groups. Hydrogen bonds were introduced, one at a time, with ideal distances and ±0.1 Å tolerance. The best combination of hydrogen bond donors and acceptors (Figure 3) increased the number of violation-free structures obtained from molecular dynamics by a factor of >3, whereas alternative hydrogen bonding schemes gave

(18) Egholm, M.; Burchardt, O.; Nielsen, P. E.; Berg, R. H. *J. Am. Chem. Soc.* **1992**, *114*, 1895−1897.
(19) (a) Bergmann, F.; Bannwarth, W.; Tam, S. *Tetrahedron Lett.* **1995**, *38*, 6823−6826. (b) Petersen, K. H.; Jensen, D. K.; Egholm, M.; Nielsen, P. E.; Burchardt, O. *Bioorg. Med. Chem. Lett.* **1995**, *5*, 1119−1124. (c) Van der Laan, A. C.; Meeuwenoord, N. J.; Khyl-Yeheskiely, E.; Oosting, R. S.; Brands, R.; van Boom, J. H. *Rec. Trav. Chim. Pays-Bas* **1995**, *114*, 295−297. (d) Stetsenko, D. A.; Lubyako, E. N.; Potapov, V. K.; Azhikina, T. L.; Sverdlov, E. D. *Tetrahedron Lett.* **1996**, *37*, 3571−3574. (e) Uhlmann, E.; Will, D. W.; Breipohl, G.; Langner, D.; Ryte, A. *Angew. Chem., Int. Ed. Engl.* **1996**, *35*, 2632−2635. (f) Van der Laan, A. C.; Havenaar, P.; Oosting, R. S.; Kuyl-Yeheskiely, E.; Uhlmann, E.; van Boom, J. H. *Bioorg. Med. Chem. Lett.* **1998**, *8*, 663−668.
(20) Westheimer, F. H. *Nature* **1987**, *235*, 1173−1178.
(21) Pons, J. L.; Malliavin, T. E.; Delsuc, M. A. *J. Biomol. NMR* **1996**, *8*, 445−452.
(22) Provided by A. T. Brünger, Yale University.
(23) Wijmenga, S. S.; Mooren, M. M. W.; Hilbers, C. W. in *NMR of Macromolecules, A Practical Approach*; Roberts, G. C. K., Ed.; Oxford University Press: Oxford, 1993; pp 217−288.
(24) Richert, C., Ph.D. Thesis, ETH Zurich, 1994.

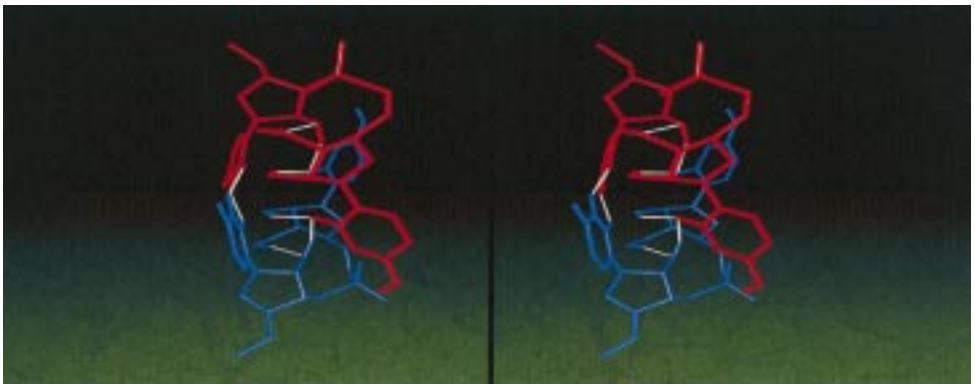

Figure 4. Stereodrawing of the core of the duplex formed by $U_{SO_2}C$. The two strands are colored red and blue. Hydrogen bonds are indicated as broken white lines. Protecting groups were omitted, but the bond connecting N4 of cytosine to the benzoyl group is shown to indicate the location of the solubilizing group. Figures 2, 3, and 4 were generated with VMD.[27]

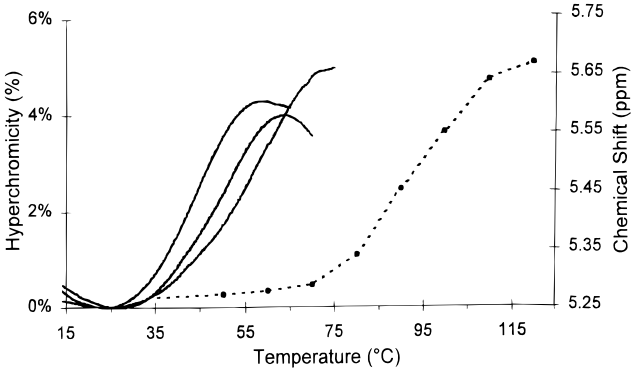

Figure 5. Composite plot of spectroscopically monitored melting transitions for $U_{SO_2}C$. Solid lines: UV hyperchromicity in $C_2H_4Cl_2$ solutions at 19 μM, 37 μM, and 70 μM strand concentration, observed at 260 nm (left *y* axis); dotted line: ^{1}H NMR chemical shifts for H5-U at 11 mM strand concentration in $C_2D_2Cl_4$ (right y axis).

substantially fewer structures and increased energies. Alternative hydrogen bonding patterns are deemed unlikely but cannot be rigorously excluded.

Generation of the back-calculated NOESY spectrum from the average structure obtained as described above revealed a number of cross-peaks to H5′/5″ and H6′/6″ of the 3′-terminal residue in the back-calculated spectrum that were unmatched in the experimental spectrum. This indicated that the internucleotide linkage partly collapsed onto the core of the structure during restrained molecular dynamics. As previously reported by Moore and collaborators for natural RNA,[25] repulsive constraints, or "Unoes" can be used to overcome such problems. In the case of $U_{SO_2}C$, three repulsive constraints with a square well energy function and an interproton distance of 8.0 ± 2.5 Å, originating from H5′/5″ or H6′/6″ of C2 and pointing to H3 of U1 or the ortho protons of the benzoyl group were introduced. Additionally, a low energy planarity constraint was introduced for the U:U base pair, which allows for the buckle and propeller twist ranges observed in oligonucleotide crystal structures. Molecular dynamics including these additional constraints produced a further increase in the yield of violation-free structures (10 out of 50) and satisfactory agreement between the experimental and the back-calculated NOESY spectrum (Figure 1a and c). This final set of refined structures retains the geometry and (within ±3%) the energy of the two violation-free structures obtained in the original calculation with distance and dihedral constraints only, but produces a larger set of structures with small root-mean-square deviation (Table 1).

UV−Vis Melting Experiments. Melting curves were acquired at 260 nm on a Perkin-Elmer Lambda 10 spectrophotometer at a heating rate of 1 °C per minute. Melting points were determined as the extrema of the 91 point first derivative using Perkin-Elmer UV TempLab, version 1.2 after smoothing curves with a 25 point moving average. At least six melting curves per concentration were acquired, giving averages with standard deviations between 0.9 and 2.5 °C. Thermodynamic parameters were determined from ln c_t versus $1/T_m$ plots (Supplementary Information) using $1/T_m = (R/\Delta H°)\ln c_t + \Delta S°/\Delta H°$, where T_m is the melting point, c_t is the total strand concentration, and R is the molar gas constant (8.3145 J mol^{-1} K^{-1}).[26]

Acknowledgment. We thank Dr. S. A. Benner, in whose laboratory $U_{SO_2}C$ was first prepared, for comments on the manuscript, B. Brandenberg (ETH Zurich) for acquisition of initial NMR spectra, J. Sudmeier for help with later NMR experiments, and M. Simon for help with van't Hoff analysis. We are grateful to Tufts University (F.R.A.C. Award) and the National Institutes of Health (Grant GM54783 to C.R.) for financial support.

Supporting Information Available: An expanded NOESY spectrum, one-dimensional ^{1}H spectra (in $CDCl_3/D_2O$ and $C_2H_2Cl_4$) at different temperatures, plots of ln c_{total} versus $1/T_m$, and coordinates of the average structure and lowest energy structure of $U_{SO_2}C$ (15 pages, print/PDF).

JA9817951

(25) (a) Stallings S. C.; Moore, P. B. *Structure* **1997**, *5*, 1173−1185. (b) Dallas, A.; Moore, P. B. *Structure* **1997**, *5*, 1639−1653.

(26) Marky, L. A.; Breslauer, K. J. *Biopolymers* **1987**, *26*, 1601−1620.

(27) Humphrey, W.; Dalke, A.; Schulten, K. *J. Mol. Graphics* **1996**, *14*, 33−38.

(28) Schindelin, H.; Zhang, M.; Bald, R.; Fürste, J.-P.; Erdmann, V. A.; Heinemann, U. *J. Mol. Biol.* **1995**, *249*, 595−603.